Beam-Spin Asymmetries in the Azimuthal Distribution of Pion Electroproduction

A. Airapetian,[16] Z. Akopov,[27] M. Amarian,[7, 27] A. Andrus,[15] E.C. Aschenauer,[7] W. Augustyniak,[26] H. Avakian*,[11] R. Avakian,[27] A. Avetissian,[27] E. Avetisyan,[11, 27] A. Bacchetta,[6] P. Bailey,[15] S. Belostotski,[19] N. Bianchi,[11] H.P. Blok,[18, 25] H. Böttcher,[7] A. Borissov,[14] A. Borysenko,[11] A. Brüll*, V. Bryzgalov,[20] M. Capiluppi,[10] G.P. Capitani,[11] G. Ciullo,[10] M. Contalbrigo,[10] P.F. Dalpiaz,[10] W. Deconinck,[16] R. De Leo,[2] M. Demey,[18] L. De Nardo,[6, 23] E. De Sanctis,[11] E. Devitsin,[17] M. Diefenthaler,[9] P. Di Nezza,[11] J. Dreschler,[18] M. Düren,[13] M. Ehrenfried,[9] A. Elalaoui-Moulay,[1] G. Elbakian,[27] F. Ellinghaus,[5] U. Elschenbroich,[12] R. Fabbri,[18] A. Fantoni,[11] L. Felawka,[23] S. Frullani,[22] A. Funel,[11] G. Gapienko,[20] V. Gapienko,[20] F. Garibaldi,[22] K. Garrow,[23] G. Gavrilov,[6, 19, 23] V. Gharibyan,[27] F. Giordano,[10] O. Grebeniouk,[19] I.M. Gregor,[7] H. Guler,[7] C. Hadjidakis,[11] K. Hafidi,[1] M. Hartig,[13] D. Hasch,[11] T. Hasegawa,[24] W.H.A. Hesselink,[18, 25] A. Hillenbrand,[9] M. Hoek,[13] Y. Holler,[6] B. Hommez,[12] I. Hristova,[7] G. Iarygin,[8] A. Ivanilov,[20] A. Izotov,[19] H.E. Jackson,[1] A. Jgoun,[19] R. Kaiser,[14] T. Keri,[13] E. Kinney,[5] A. Kisselev,[5, 19] T. Kobayashi,[24] M. Kopytin,[7] V. Korotkov,[20] V. Kozlov,[17] B. Krauss,[9] P. Kravchenko,[19] V.G. Krivokhijine,[8] L. Lagamba,[2] L. Lapikás,[18] P. Lenisa,[10] P. Liebing,[7] L.A. Linden-Levy,[15] W. Lorenzon,[16] J. Lu,[23] S. Lu,[13] B.-Q. Ma,[3] B. Maiheu,[12] N.C.R. Makins,[15] Y. Mao,[3] B. Marianski,[26] H. Marukyan,[27] F. Masoli,[10] V. Mexner,[18] N. Meyners,[6] T. Michler,[9] O. Mikloukho,[19] C.A. Miller,[23] Y. Miyachi,[24] V. Muccifora,[11] M. Murray,[14] A. Nagaitsev,[8] E. Nappi,[2] Y. Naryshkin,[19] M. Negodaev,[7] W.-D. Nowak,[7] K. Oganessyan,[6, 11] H. Ohsuga,[24] A. Osborne,[14] R. Perez-Benito,[13] N. Pickert,[9] M. Raithel,[9] D. Reggiani,[9] P.E. Reimer,[1] A. Reischl,[18] A.R. Reolon,[11] C. Riedl,[9] K. Rith,[9] G. Rosner,[14] A. Rostomyan,[6] L. Rubacek,[13] J. Rubin,[15] D. Ryckbosch,[12] Y. Salomatin,[20] I. Sanjiev,[1, 19] I. Savin,[8] A. Schäfer,[21] G. Schnell,[12] K.P. Schüler,[6] J. Seele,[5] R. Seidl,[9] B. Seitz,[13] C. Shearer,[14] T.-A. Shibata,[24] V. Shutov,[8] K. Sinram,[6] M. Stancari,[10] M. Statera,[10] E. Steffens,[9] J.J.M. Steijger,[18] H. Stenzel,[13] J. Stewart,[7] F. Stinzing,[9] J. Streit,[13] P. Tait,[9] H. Tanaka,[24] S. Taroian,[27] B. Tchuiko,[20] A. Terkulov,[17] A. Trzcinski,[26] M. Tytgat,[12] A. Vandenbroucke,[12] P.B. van der Nat,[18] G. van der Steenhoven,[18] Y. van Haarlem,[12] V. Vikhrov,[19] C. Vogel,[9] S. Wang,[3] Y. Ye,[4] Z. Ye,[6] S. Yen,[23] B. Zihlmann,[12] and P. Zupranski[26]

(The HERMES Collaboration)

[1]*Physics Division, Argonne National Laboratory, Argonne, Illinois 60439-4843, USA*
[2]*Istituto Nazionale di Fisica Nucleare, Sezione di Bari, 70124 Bari, Italy*
[3]*School of Physics, Peking University, Beijing 100871, China*
[4]*Department of Modern Physics, University of Science and Technology of China, Hefei, Anhui 230026, China*
[5]*Nuclear Physics Laboratory, University of Colorado, Boulder, Colorado 80309-0390, USA*
[6]*DESY, 22603 Hamburg, Germany*
[7]*DESY, 15738 Zeuthen, Germany*
[8]*Joint Institute for Nuclear Research, 141980 Dubna, Russia*
[9]*Physikalisches Institut, Universität Erlangen-Nürnberg, 91058 Erlangen, Germany*
[10]*Istituto Nazionale di Fisica Nucleare, Sezione di Ferrara and Dipartimento di Fisica, Università di Ferrara, 44100 Ferrara, Italy*
[11]*Istituto Nazionale di Fisica Nucleare, Laboratori Nazionali di Frascati, 00044 Frascati, Italy*
[12]*Department of Subatomic and Radiation Physics, University of Gent, 9000 Gent, Belgium*
[13]*Physikalisches Institut, Universität Gießen, 35392 Gießen, Germany*
[14]*Department of Physics and Astronomy, University of Glasgow, Glasgow G12 8QQ, United Kingdom*
[15]*Department of Physics, University of Illinois, Urbana, Illinois 61801-3080, USA*
[16]*Randall Laboratory of Physics, University of Michigan, Ann Arbor, Michigan 48109-1040, USA*
[17]*Lebedev Physical Institute, 117924 Moscow, Russia*
[18]*Nationaal Instituut voor Kernfysica en Hoge-Energiefysica (NIKHEF), 1009 DB Amsterdam, The Netherlands*
[19]*Petersburg Nuclear Physics Institute, St. Petersburg, Gatchina, 188350 Russia*
[20]*Institute for High Energy Physics, Protvino, Moscow region, 142281 Russia*
[21]*Institut für Theoretische Physik, Universität Regensburg, 93040 Regensburg, Germany*
[22]*Istituto Nazionale di Fisica Nucleare, Sezione Roma 1, Gruppo Sanità and Physics Laboratory, Istituto Superiore di Sanità, 00161 Roma, Italy*
[23]*TRIUMF, Vancouver, British Columbia V6T 2A3, Canada*
[24]*Department of Physics, Tokyo Institute of Technology, Tokyo 152, Japan*
[25]*Department of Physics and Astronomy, Vrije Universiteit, 1081 HV Amsterdam, The Netherlands*
[26]*Andrzej Soltan Institute for Nuclear Studies, 00-689 Warsaw, Poland*
[27]*Yerevan Physics Institute, 375036 Yerevan, Armenia*
(Dated: April 24, 2007)

A measurement of the beam-spin asymmetry in the azimuthal distribution of pions produced in semi-inclusive deep-inelastic scattering off protons is presented. The measurement was performed us-

ing the HERMES spectrometer with a hydrogen gas target and the longitudinally polarized 27.6 GeV positron beam of HERA. The sinusoidal amplitude of the dependence of the asymmetry on the angle ϕ of the hadron production plane around the virtual photon direction relative to the lepton scattering plane was measured for π^+, π^- and π^0 mesons. The dependence of this amplitude on the Bjorken scaling variable and on the pion fractional energy and transverse momentum is presented. The results are compared to theoretical model calculations.

Single-spin asymmetries (SSA) in semi-inclusive deep-inelastic scattering (SIDIS) are known as a powerful tool to probe the partonic structure of the nucleon. If the orbital motion of the quarks is neglected, the structure of nucleon can be described in the leading twist by 3 parton distribution functions (PDF) defining the momentum f_1, helicity g_1, and transversity h_1 distributions. The observation of different azimuthal asymmetries and, in particular SSAs were an indication of a more complex inner structure of the nucleon. Those effects were recognized to be due to correlations of spin and transverse momentum of quarks and/or hadrons and appear as moments of the azimuthal angle between scattering and production planes. The $\sin \phi$ azimuthal moments contain contributions from different chiral-odd and/or naïve *time-reversal-odd* (T-odd) distribution and fragmentation functions, arising from interference of wave functions for different orbital angular momentum states and final state interactions [1–10]. Experimentally correlations between spin and transverse momentum either in the initial target nucleon (e.g. the Sivers mechanism [11]) or in the fragmentation process (e.g. the Collins mechanism [12]) result in an asymmetry of the distribution of hadrons around the virtual photon direction. Asymmetries are attractive observables as they are expected to be less sensitive to a number of higher order corrections than cross sections measured in SIDIS [13]. SSAs in production of pseudoscalar mesons were studied with both longitudinally [14–16] and transversely [17, 18] polarized targets. Recently, SSAs have been observed also in SIDIS with longitudinal polarized beams and unpolarized targets (in the following refered to as beam SSAs) [14, 19].

Under the assumption of factorization [20, 21], the general expression for the SIDIS cross section σ can be given as convolutions of distribution functions $f^{H \to q}$ (DF), elementary hard scattering cross section $\sigma^{eq \to eq}$, and fragmentation functions $D^{q \to h}$ (FF),

$$\sigma^{eH \to ehX} = f^{H \to q} \otimes \sigma^{eq \to eq} \otimes D^{q \to h}. \qquad (1)$$

In the particular case of a longitudinally polarized beam (L) and an unpolarized target (U), and in the limit of massless quarks, the differential polarized cross section
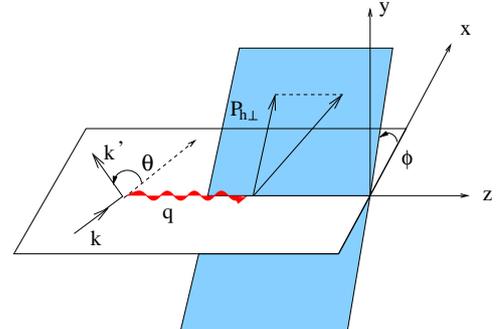
*Present address: Thomas Jefferson National Accelerator Facility, Newport News, Virginia 23606, USA

FIG. 1: Definition of kinematic planes for semi-inclusive deep-inelastic scattering.

σ_{LU} can be written as a sum of convolutions of twist-2 and twist-3 functions [22, 23]

$$\frac{d^5\sigma_{LU}}{dx\,dy\,dz\,d\phi\,dP_{h\perp}^2} \propto \lambda_e \sin \phi\, y \sqrt{1-y} \frac{M}{Q} \times$$

$$\int d^2\boldsymbol{p_T}\, d^2\boldsymbol{k_T}\, \delta^{(2)}\Big(\boldsymbol{p_T} - \frac{\boldsymbol{P_{h\perp}}}{z} - \boldsymbol{k_T}\Big)$$

$$\Bigg\{ \frac{\hat{\boldsymbol{P}}_{\boldsymbol{h}\perp} \cdot \boldsymbol{p_T}}{M} \Big[\frac{M_h}{Mz} h_1^\perp E + x\, g^\perp D_1 \Big] -$$

$$\frac{\hat{\boldsymbol{P}}_{\boldsymbol{h}\perp} \cdot \boldsymbol{k_T}}{M_h} \Big[\frac{M_h}{Mz} f_1\, G^\perp + x\, e H_1^\perp \Big] \Bigg\}. \qquad (2)$$

In Eq. 2, λ_e is the lepton helicity, M and M_h are the nucleon and hadron masses, $-Q^2$ is the 4-momentum transfer squared, $\boldsymbol{P_{h\perp}}$ is the transverse momentum of the detected hadron with $\hat{\boldsymbol{P}}_{\boldsymbol{h}\perp} = \boldsymbol{P_{h\perp}}/|\boldsymbol{P_{h\perp}}|$, $\boldsymbol{p_T}$ ($\boldsymbol{k_T}$) is the intrinsic quark transverse momentum in the generic distribution function f (fragmentation function D), $E(E')$ and E_h are the energies of the incoming(scattered) lepton and the hadron produced, ν is the energy of the virtual photon and the azimuthal angle ϕ is defined as the angle between the lepton-scattering and hadron-production planes according to the Trento convention [24]. See Fig. 1 for the definition of the kinematic planes, where k (k') is the four-momentum of the incoming (scattered) lepton and q that of the virtual photon. In Eq. 2, a charge-weighted sum over quark and antiquark flavours is implicit. The quantities f_1 and D_1 are the twist-2 DF and FF, which appear in the unpolarized cross-section when integrated over ϕ

$$\frac{d^3\sigma_{UU}}{dx\,dy\,dz} \propto (1 - y + y^2/2) f_1(x) D_1(z). \qquad (3)$$

In Eq. 2, e is a chiral-odd twist-3 unpolarized DF [25] that can be related to the pion-nucleon σ-term, which in its turn is related to the strangeness content of the nucleon [26]. The T-odd DF e is convolved with the twist-2 Collins FF $H_1^\perp$, which also appears in longitudinal and transverse target-spin asymmetries [17]. Another contribution is given by the twist-2 DF $h_1^\perp$ (Boer-Mulders DF [8]), which is interpreted as representing the correlation between the transverse spin and intrinsic transverse momentum of a quark in an unpolarized nucleon. Here it is convolved with the twist-3 chiral-odd FF E [27, 28]. The remaining terms contain the twist-3 DF $g^\perp$ and FF $G^\perp$ convolved with the unpolarized FF and DF, respectively. The DF $g^\perp$ can be directly accessed through a measurement of the beam-spin asymmetry in jet production [22, 29]. Since the beam SSA has no leading-twist contribution (cf. Eq. 2) it is expected to be accessible only at moderate values of Q^2.

In this paper we present a measurement of the beam SSA for charged and neutral pions produced in SIDIS at HERMES during the years 1996-2000. The results presented supercede a previous HERMES measurement of the beam SSA for π^+ [14] by almost doubling the statistics, which allowed the extraction of the kinematic dependences of the beam SSA on z, x and $P_{h\perp}$ and the addition of a measurement for π^- and π^0 mesons. The experiment used the polarized positron beam of the HERA accelerator and a hydrogen gas target. Positrons with an energy of 27.6 GeV were scattered off hydrogen nuclei in an atomic gas target [30]. The beam was polarized in the transverse direction due to the Sokolov-Ternov effect [31]. Longitudinal orientation of the beam spin was obtained by using a pair of spin rotators located before and behind the interaction region of HERMES. The beam helicity was flipped every few months. The beam polarization was measured by two independent HERA polarimeters [32] and had an average value of 0.53 with a fractional systematic uncertainty of 2.9%. The target mode was either unpolarized or longitudinally polarized with a fast (90 s) helicity flip. The resulting target polarization in the analyzed sample was $-1.3 \cdot 10^{-4}$, which is consistent with zero and was safely ignored in the analysis. The scattered positrons and associated hadrons were detected by the HERMES spectrometer [33]. Positrons were distinguished from hadrons by the use of a set of particle identification detectors: a transition-radiation detector, a preshower radiator/hodoscope, a threshold Čerenkov detector (upgraded to a RICH detector [34] in 1998) and an electromagnetic calorimeter [35]. The average positron identification efficiency exceeded 98% with a hadron contamination in the positron sample below 1%. Several kinematic requirements were imposed on the scattered positron, namely $1 < Q^2 < 15$ GeV^2, $0.023 < x < 0.4$, $W^2 > 4$ GeV^2, $y < 0.85$.

For identification of charged pions the Čerenkov and RICH detectors were used during the corresponding data taking periods. To assure reliable identification of pions in both detectors the momentum range of $4.5 < P < 13.5$
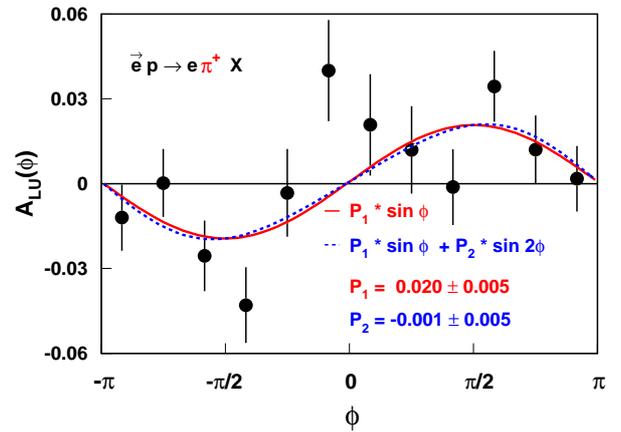

FIG. 2: Beam SSA as a function of ϕ for π^+ electroproduction at mid-z range. The solid curve represents a $\sin\phi$ fit, and the dashed one includes also the $\sin 2\phi$ harmonic. Only statistical errors are shown.

GeV was chosen.

Neutral pions were identified requiring two neutral clusters in the electromagnetic calorimeter with energies above a threshold of 1 GeV. A peak around the π^0 mass of 0.135 GeV with a resolution of about 0.012 GeV was clearly observed in the invariant mass $M_{\gamma\gamma}$ distribution of all photon pairs. Neutral pions were selected requiring $0.11 < M_{\gamma\gamma} < 0.16$ GeV. By fitting the $M_{\gamma\gamma}$ distribution with a Gaussian plus a polynomial of third order, the combinatorial background was estimated to be up to 35% in the lower-z region and negligible ($< 5\%$) for $z > 0.5$. A momentum cut of $P > 2$ GeV was used to reduce the low-energetic combinatorial background. The spatial granularity of the electromagnetic calorimeter imposes an upper limit of about $P < 15$ GeV on the π^0 momenta.

The dependence of the cross-section asymmetry on the azimuthal angle ϕ was extracted as

$$A_{LU}(\phi) = \frac{1}{|P_B|} \frac{\overrightarrow{N}(\phi) - \overleftarrow{N}(\phi)}{\overrightarrow{N}(\phi) + \overleftarrow{N}(\phi)}, \qquad (4)$$

where $|P_B|$ is the average absolute luminosity-weighted beam polarization, $\rightarrow$ ($\leftarrow$) denotes positive (negative) helicity of the beam and $\overrightarrow{N}$ ($\overleftarrow{N}$) is the number of selected events with a detected pion for each beam spin state normalized to DIS. The cross-section asymmetry dependence on ϕ for π^+ mesons is shown in Fig. 2 at mid-z range with mean kinematic values ($0.5 < z < 0.8$): $\langle z \rangle = 0.62$, $\langle x \rangle = 0.10$, $\langle Q^2 \rangle = 2.55$ GeV^2, and $\langle P_{h\perp} \rangle = 0.45$ GeV. Fourier amplitudes were extracted with fits using the functions $p_1 \cdot \sin\phi$ and $p_1 \cdot \sin\phi + p_2 \cdot \sin 2\phi$, also shown in the figure. For both fits the resulting asymmetry amplitude $A_{LU}^{\sin\phi}$ equals 0.020 ± 0.005. The amplitude $A_{LU}^{\sin 2\phi}$ is compatible with zero.

The amplitudes $A_{LU}^{\sin\phi}$ for all pions are shown in Fig. 3 and Table I as a function of z, x, and $P_{h\perp}$. Three regions in z are considered: the low-z ($0.2 < z < 0.5$), the mid-z ($0.5 < z < 0.8$), and the high-z region ($0.8 < z < 1$). In the latter region the contributions of exclusive processes become sizeable. The distributions of $A_{LU}^{\sin\phi}$ in x and $P_{h\perp}$ are extracted for the low- and mid-z regions separately and presented as open and full circles, respectively.

The sources of systematic uncertainties are the beam polarization measurement with an average relative uncertainty on the asymmetry of 5.5%, radiative processes, acceptance effects, asymmetry amplitude extraction method and the hadron identification efficiency. The combined systematic uncertainty, excluding the contribution from the beam polarization measurement, was evaluated by Monte Carlo studies and found to be less than 0.005 in total.

For the determination of the π^0 asymmetries, the asymmetry of the combinatorial background A_{LU}^{bg} was measured outside the mass window of the π^0 peak and found to equal about 0.03 on average. Since the contribution from the combinatorial background is negligible in the mid- and high-z regions, a systematic uncertainty due to combinatorial background subtraction adds to the total systematic uncertainty in the low-z region reaching 0.007. The measured asymmetry A_{LU}^{meas} was corrected in each kinematic bin using the equation

$$A_{LU}^{corr} = \frac{A_{LU}^{meas}N_{meas} - A_{LU}^{bg}N_{bg}}{N_{meas} - N_{bg}}, \tag{5}$$

where N_{meas} and N_{bg} are the number of photon pairs in the region considered in the invariant mass distribution and uncorrelated photon pairs, respectively.

The amplitude $A_{LU}^{\sin\phi}$ for π^+ mesons is found to be positive on average. It is compatible with zero in the low-z region and exhibits a rise to values of about 0.02 for increasing z. The x and $P_{h\perp}$ dependences of the amplitude are consistent with zero in the low-z region whereas in the mid-z region they decrease at large x and $P_{h\perp}$.

The amplitude $A_{LU}^{\sin\phi}$ for π^- mesons is consistent with zero in the whole z range, with fluctuations around zero in the x and $P_{h\perp}$ distributions.

The asymmetry for π^0 mesons is positive and of the order of about 0.03 in the whole z range except in the highest and lowest bins where the asymmetry is compatible with zero. The dependence of the asymmetry amplitude on x is weak while for $P_{h\perp}$ the amplitude decreases at higher $P_{h\perp}$.

Semi-inclusive pion production ($ep \rightarrow e'\pi X$) with an underlying mechanism of quark fragmentation is diluted by exclusive vector meson (VM) production which can contribute significantly in certain kinematic regions at HERMES. In Fig. 4 (lower panel) the relative contribution of exclusive VM production in the semi-inclusive pion sample is shown as obtained with the PYTHIA Monte Carlo generator tuned for HERMES kinematics [36]. The
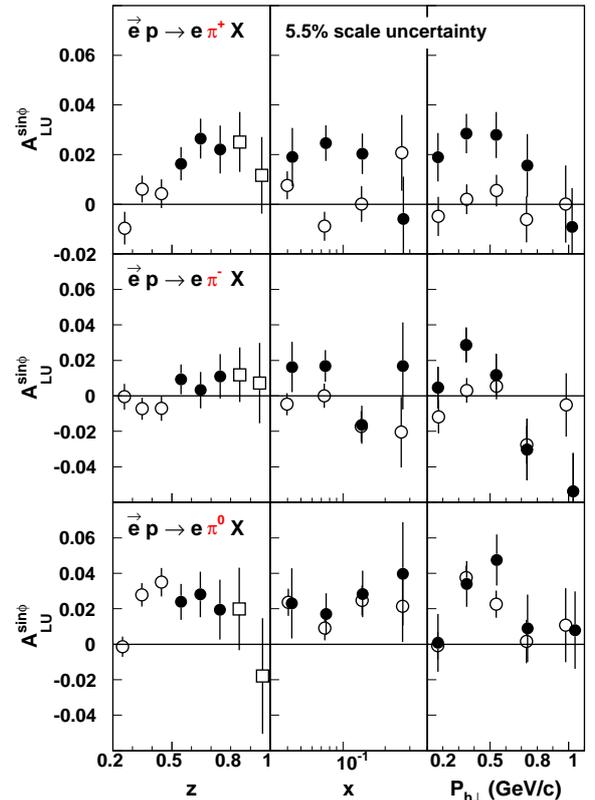

FIG. 3: Dependence of the beam SSA on z, x, and $P_{h\perp}$. Results for the x and $P_{h\perp}$ dependences are presented separately for the low-z ($0.2 < z < 0.5$) and mid-z ($0.5 < z < 0.8$) regions, indicated by open and full circles, respectively. For the high-z ($0.8 < z < 1$, open squares) region only the z dependence is pictured. The error bars represent the statistical uncertainty. An additional 5.5% fractional scale uncertainty is due to the systematic uncertainty in the beam polarization measurement. Total systematic uncertainties do not exceed 0.005.

VM contribution increases with z from about 4% in the lowest z-bin to approximately 40%(60%) in the highest z-bin for the $\pi^+(\pi^-)$ mesons. The π^0 meson sample is less contaminated with VM decay products since the ω meson production rate is very small at HERMES energies; hence its contribution to the π^0 sample does not exceed 5% in the kinematic range considered.

To assess the effect of the exclusive processes, the amplitude $A_{LU}^{\sin\phi}$ has been extracted for pions identified as decay products of exclusive ρ^0 mesons in the data, and compared with a Monte Carlo simulation based on the VMD model and spin-density matrix elements extracted from HERMES data [37]. The asymmetry as a function of z extracted for π^+ from the Monte Carlo and the data is presented in Fig. 4 (upper panel). Due to the symmetric decay of the ρ^0 mesons the asymmetry amplitudes of π^- and π^+ mesons are identical. The agreement between
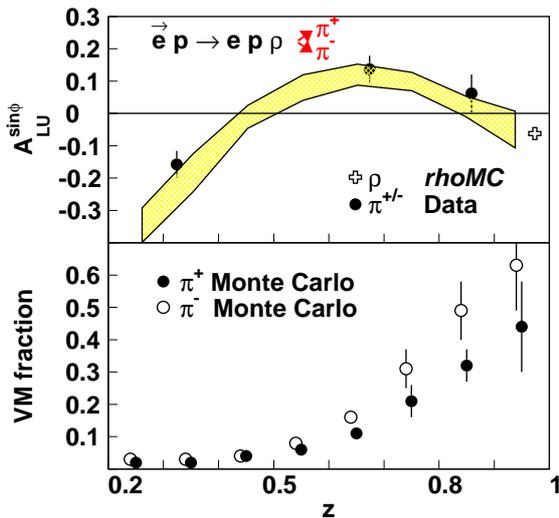
FIG. 4: Top panel: amplitude $A_{LU}^{\sin\phi}$ for π^+ mesons originating from ρ^0 meson decays, obtained with Monte Carlo (band) and data (full circles). The open cross displays the asymmetry for the ρ^0 itself (Monte Carlo). Bottom panel: the fraction of pions in the SIDIS sample originating from VM decays.
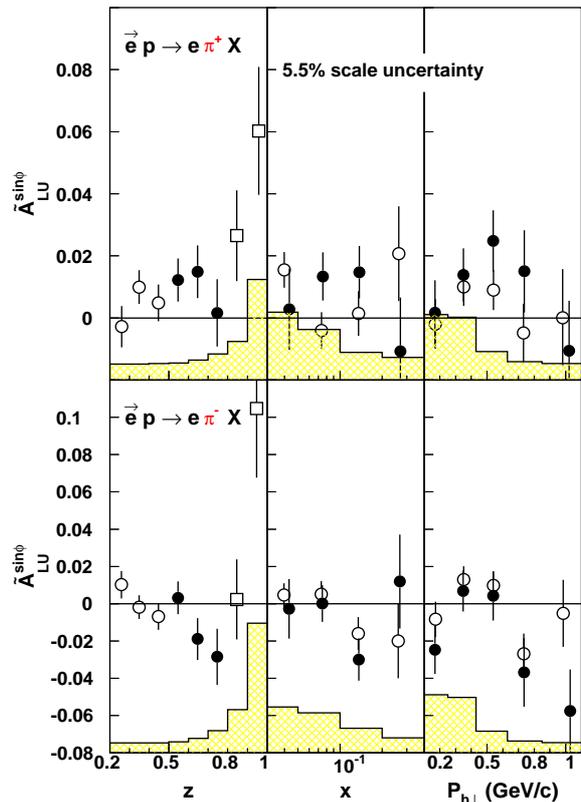

FIG. 5: Dependence of $\widetilde{A}_{LU}^{\sin\phi}$ on z, x and $P_{h\perp}$ for charged pions. The contribution from VM decays has been determined from a Monte Carlo simulation and subsequently subtracted from the asymmetries. The measurement of the x and $P_{h\perp}$ dependences is made separately for low ($0.2 < z < 0.5$) and middle ($0.5 < z < 0.8$) z-ranges (indicated by open and full circles, respectively). The error band indicates the uncertainties from PYTHIA and RHOMC.

data and Monte Carlo within the available statistical accuracy is clearly visible.

The information obtained from the Monte Carlo simulation was used to subtract the contribution from exclusive VM production to the measured asymmetry amplitudes $A_{LU}^{\sin\phi}$. The subtraction was performed similarly to the combinatorial background correction in the π^0 meson sample (cf. Eq. 5). The corrected asymmetry $\widetilde{A}_{LU}^{\sin\phi}$ is presented in Fig. 5 for charged pions. The asymmetry is roughly constant at about 0.01 for π^+ and compatible with zero for π^- in the low and middle range of z and exhibits a steep rise in the highest z bins for both π^+ and π^-. The uncertainties from PYTHIA and RHOMC Monte Carlo generators are included in the systematic error band.

A similar measurement [19] has been performed for π^+ mesons by the CLAS collaboration at JLab at a lower beam energy (4.3 GeV), higher average x ($\langle x\rangle \simeq 0.3$) and lower average Q^2 ($\langle Q^2\rangle \simeq 1.55$ GeV^2). The comparison of the HERMES and CLAS measurements of $A_{LU}^{\sin\phi}$ as a function of z is shown for π^+ in Fig. 6. No correction for VM contribution was applied. In order to account for the different kinematic ranges of the two experiments, both $A_{LU}^{\sin\phi}$ amplitudes are scaled by an $\langle Q\rangle/f(y)$ kinematic prefactor (cf. Eq. 2 and 3), where

$$f(y) = \frac{y\sqrt{1-y}}{(1-y+y^2/2)} \qquad . \qquad (6)$$

The $f(y)$ scaled asymmetries are also often referred to as *virtual photon asymmetries* in contrast to the usual

lepton beam asymmetries. A previous HERMES measurement [14] in the range $0.2 < z < 0.7$ is added for completeness. The agreement between the two measurements at different beam energies indicates that the beam SSA does not exhibit a strong dependence neither on the incoming lepton energy nor on x.

Several theoretical models [10, 26–29] have been developed to describe the beam SSA measurements. In Fig. 7 the $A_{LU}^{\sin\phi}$ asymmetry amplitudes of π^+ mesons are compared to two model predictions. The solid curve represents a quark-diquark model calculation [27], which claims a dominant contribution from the $eH_1^\perp$ term over the $h_1^\perp E$ term (cf. Eq. 2). In contrast, the dashed curve is a calculation using the chiral quark model [28] under the assumption that the asymmetry arises solely from the $h_1^\perp E$ term. Both models neglect the contribution of the remaining terms in Eq. 2. The full circles represent the measurement of the beam SSA for π^+ mesons and the empty squares the asymmetry amplitudes $\widetilde{A}_{LU}^{\sin\phi}$ cor-
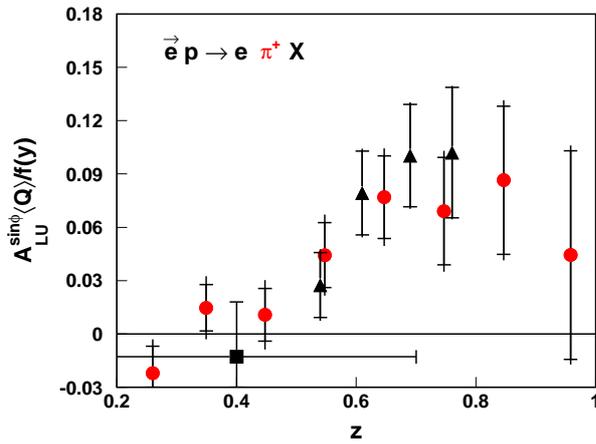
FIG. 6: Comparison of the kinematically rescaled asymmetry amplitudes $A_{LU}^{\sin\phi} \cdot \langle Q\rangle/f(\langle y\rangle)$ for π^+ between the HERMES (circles) and CLAS (triangles) measurements. The full square represents a previous HERMES measurement [14], averaged over the indicated large z range ($0.2 < z < 0.7$). The outer error bars represent the quadratic sum of the systematic uncertainty and the statistical uncertainty (inner error bars).

FIG. 7: Comparison of the π^+ amplitude uncorrected $A_{LU}^{\sin\phi}$ (full circles) and corrected $\widetilde{A}_{LU}^{\sin\phi}$ (open squares) for VM contribution with model predictions. Outer error bars represent the uncertainties introduced by VM subtraction. A fractional scale uncertainty of 5.5% and a systematic uncertainty of 0.005 are common. The solid curve represents the quark-diquark model [27], and the dashed curve the chiral quark model [28].

rected for the contribution from the decay of exclusively produced VMs. Both models describe the data in the low and middle z-range equally well, while in the higher z-range, where the influence of the exclusive processes in the data increases, the models diverge. In the high-z range the quark-diquark model is in better agreement with the uncorrected asymmetry amplitudes while the corrected asymmetry amplitudes exhibit a rise at high z that is described better by the chiral quark model prediction. Since the models are not reliable in the high-z range such a comparison should be treated carefully, and doesn't allow to explicitly rule out any of the models with the available statistical accuracy.

In [29] the $A_{LU}^{\sin(\phi)}$ amplitude is calculated within a simple quark-diquark model with a final state gluon exchange without requiring the quarks to have spin. There the contribution of the $g^\perp$ term is considered and the resulting asymmetry compared to the measurements from [19] and preliminary HERMES data on asymmetry amplitude dependence on x. In addition, a pQCD based calculation predicting such asymmetries at a per mille level [38] should be noted.

In conclusion, beam-spin asymmetry amplitudes $A_{LU}^{\sin\phi}$ have been measured in the azimuthal distribution of pions produced in semi-inclusive DIS. The amplitudes $A_{LU}^{\sin\phi}$ for π^+ are consistent with zero for low z and exhibit a rise with increasing z, reaching values of about 0.02. This result is in reasonable agreement with calculations based on quark-diquark and chiral quark models, as well as with data measured previously at different kinematics. The comparison with the latter gives no experimental evidence for a strong dependence of the amplitudes $A_{LU}^{\sin\phi}$
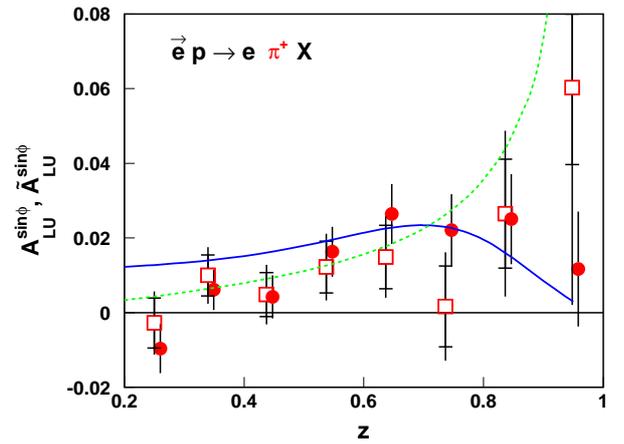
on the beam energy.

The results of the first measurement of $A_{LU}^{\sin\phi}$ for negative pions are consistent with zero within the available statistical accuracy. The asymmetry for neutral pions is roughly constant and of the order of 0.03, decreasing to zero only in the lowest and highest z regions.

The variety of components in the polarized cross-section (c.f. Eq. 2) make it difficult to disentangle them and find a dominant source of the beam-spin asymmetry. Two theoretical models which both describe the data well are based on opposite assumptions. Other models which do not include the quark spin degrees of freedom predict sizeable asymmetries. It would be interesting to extend these studies to double-hadron production integrated over the transverse momentum of the hadron pair as there all terms in Eq. 2 that explicitly require intrinsic transverse momentum vanish [39].

The contribution of exclusive VM production to the SIDIS asymmetries observed indicates that a proper investigation of the hadron production process through fragmentation requires a good knowledge of exclusive meson production mechanisms and corresponding asymmetries. The latter have been investigated using experimental data and Monte Carlo simulations. They were used to obtain the asymmetry amplitudes for pions produced in the fragmentation process in SIDIS without contamination by vector mesons.

In a global analysis the beam SSA combined with longitudinal and transverse target spin asymmetries in single- and double-hadron production, as well as jet asymmetries, if available, will allow a more complete understand-

TABLE I: Beam SSA: z, x, and $P_{h\perp}$ dependences of $A_{LU}^{\sin\phi}$ and $\widetilde{A}_{LU}^{\sin\phi}$ for charged and neutral pions. The systematic uncertainty induced by VM subtraction is given as $\widetilde{\Delta}_{vm}^{\pi^\pm}$. An additional 5.5% scale uncertainty is due to the beam polarization measurement. Other systematic uncertainties do not exceed 0.005.

$\langle z\rangle$	$\langle x\rangle$	$\langle P_{h\perp}\rangle$	$\langle Q^2\rangle$	$A_{LU}^{\sin\phi,\pi^+} \pm \Delta_{stat}^{\pi^+}$	$A_{LU}^{\sin\phi,\pi^-} \pm \Delta_{stat}^{\pi^-}$	$A_{LU}^{\sin\phi,\pi^0} \pm \Delta_{stat}^{\pi^0}$	$\widetilde{A}_{LU}^{\sin\phi,\pi^+} \pm \widetilde{\Delta}_{stat}^{\pi^+} \pm \widetilde{\Delta}_{vm}^{\pi^+}$	$\widetilde{A}_{LU}^{\sin\phi,\pi^-} \pm \widetilde{\Delta}_{stat}^{\pi^-} \pm \widetilde{\Delta}_{vm}^{\pi^-}$
0.26	0.065	0.40	2.29	-0.009 ± 0.006	-0.001 ± 0.007	0.002 ± 0.006	0.003 ± 0.006 ± 0.005	0.012 ± 0.007 ± 0.005
0.34	0.082	0.45	2.53	0.006 ± 0.005	-0.007 ± 0.006	0.028 ± 0.006	0.013 ± 0.005 ± 0.005	0.001 ± 0.006 ± 0.005
0.44	0.092	0.46	2.55	0.004 ± 0.005	-0.007 ± 0.006	0.035 ± 0.008	0.005 ± 0.005 ± 0.005	-0.007 ± 0.007 ± 0.005
0.54	0.098	0.47	2.51	0.016 ± 0.006	0.009 ± 0.008	0.025 ± 0.009	0.011 ± 0.006 ± 0.005	0.000 ± 0.008 ± 0.006
0.64	0.104	0.47	2.47	0.026 ± 0.007	0.003 ± 0.009	0.028 ± 0.012	0.012 ± 0.008 ± 0.006	-0.018 ± 0.010 ± 0.008
0.74	0.108	0.47	2.37	0.021 ± 0.009	0.011 ± 0.011	0.020 ± 0.015	0.000 ± 0.010 ± 0.008	-0.023 ± 0.013 ± 0.011
0.84	0.117	0.46	2.27	0.024 ± 0.010	0.013 ± 0.014	0.019 ± 0.020	0.026 ± 0.013 ± 0.012	0.003 ± 0.019 ± 0.023
0.95	0.128	0.45	2.20	0.011 ± 0.013	0.007 ± 0.020	-0.018 ± 0.030	0.065 ± 0.019 ± 0.032	0.099 ± 0.033 ± 0.069
0.62	0.043	0.53	1.30	0.019 ± 0.010	0.016 ± 0.013	0.025 ± 0.018	0.002 ± 0.012 ± 0.022	-0.007 ± 0.015 ± 0.024
0.63	0.075	0.44	1.84	0.024 ± 0.006	0.017 ± 0.008	0.016 ± 0.010	0.012 ± 0.007 ± 0.016	-0.001 ± 0.009 ± 0.021
0.62	0.137	0.42	3.19	0.020 ± 0.007	-0.016 ± 0.009	0.030 ± 0.012	0.012 ± 0.008 ± 0.009	-0.030 ± 0.010 ± 0.013
0.62	0.269	0.43	6.08	-0.005 ± 0.015	0.018 ± 0.022	0.037 ± 0.03	-0.012 ± 0.016 ± 0.007	0.009 ± 0.023 ± 0.008
0.62	0.108	0.17	2.44	0.019 ± 0.009	0.004 ± 0.01	0.000 ± 0.015	0.001 ± 0.009 ± 0.021	-0.025 ± 0.012 ± 0.031
0.62	0.105	0.35	2.45	0.028 ± 0.007	0.028 ± 0.009	0.035 ± 0.012	0.013 ± 0.008 ± 0.020	0.006 ± 0.010 ± 0.030
0.62	0.103	0.54	2.52	0.027 ± 0.008	0.012 ± 0.010	0.049 ± 0.013	0.024 ± 0.009 ± 0.009	0.004 ± 0.012 ± 0.011
0.61	0.095	0.74	2.49	0.015 ± 0.011	-0.030 ± 0.016	0.009 ± 0.018	0.015 ± 0.012 ± 0.006	-0.036 ± 0.017 ± 0.006
0.61	0.084	1.02	2.39	-0.009 ± 0.014	-0.054 ± 0.020	0.005 ± 0.020	-0.010 ± 0.014 ± 0.005	-0.058 ± 0.020 ± 0.005

ing of the nucleon structure as well as the underlying mechanisms of the quark fragmentation.

[1] A. Kotzinian, Nucl. Phys. **B441** (1995) 234.
[2] M. Anselmino, A. Efremov and E. Leader, Phys. Rept. **261**, 1 (1995)
[3] P. Mulders, R.D. Tangerman, Nucl. Phys. **B461** (1996) 197.
[4] A.V. Belitsky, X. Ji, F. Yuan, Nucl. Phys. **B656** (2003) 165.
[5] A. Belitsky, D. Muller, Phys. Lett. **B513** (2001) 349.
[6] X. Ji, J.-P. Ma, F. Yuan, Phys. Rev. **D71** (2005) 034005.
[7] R. L. Jaffe, X.-D. Ji, Nucl. Phys. **B375** (1992) 527.
[8] D. Boer, P. J. Mulders, Phys. Rev. **D57** (1998) 5780.
[9] A. De Rujula, J.M. Kaplan, E. De Rafael, Nucl. Phys. **B35** (1971) 365.
[10] A. Metz and M. Schlegel, Eur. Phys. J. A **22** (2004) 489
[11] D. W. Sivers, Phys. Rev. **D41** (1990) 83, and Phys. Rev. **D 43** (1991) 261.
[12] J. Collins, Nucl. Phys. **B396** (1993) 161.
[13] A. Bacchetta et al., Phys. Rev. **D65** (2002) 094021.
[14] A. Airapetian et al., Phys. Rev. Lett. **84** (2000) 4047.
[15] A. Airapetian et al., Phys. Rev. **D64** (2001) 097101.
[16] A. Airapetian et al., Phys. Lett. **B562** (2003) 182.
[17] A. Airapetian et al., Phys. Rev. Lett. **94** (2005) 012002.
[18] V. Yu. Alexakhin et al., Phys. Rev. Lett. **94** (2005) 202002.
[19] H. Avakian et al., Phys. Rev. **D69** (2004) 112004.
[20] J. C. Collins, L. Frankfurt, M. Strikman, Phys. Rev. **D56** (1997) 2982.
[21] X. d. Ji, J. P. Ma and F. Yuan, Phys. Lett. B **597** (2004)

299

[22] A. Bacchetta, P. J. Mulders, F. Pijlman, Phys. Lett. **B595** (2004) 309.

[23] A. Bacchetta, M. Diehl, K. Goeke, A. Metz, P. Mulders and M. Schlegel, arXiv:hep-ph/0611265.

[24] A. Bacchetta, U. D'Alesio, M. Diehl, C. A. Miller, Phys. Rev. **D70** (2004) 117504.

[25] J. Levelt, P. J. Mulders, Phys. Lett. **B338** (1994) 357.

[26] A. V. Efremov, K. Goeke, P. Schweitzer, Phys. Rev. **D67** (2003) 114014.

[27] L. P. Gamberg, D. S. Hwang, K. A. Oganessyan, Phys. Lett. **B584** (2004) 276.

[28] F. Yuan, Phys. Lett. **B589** (2004) 28.

[29] A. Afanasev, C. E. Carlson, hep-ph/0603269.

[30] A. Airapetian et al., Nucl. Instr. and Meth. **A540** (2005) 68.

[31] A. A. Sokolov, I. M. Ternov, Sov. Phys. Doklady **8** (1964) 1203.

[32] M. Beckmann et al., Nucl. Instr. and Meth. **A479** (2002) 334.

[33] K. Ackerstaff et al., Nucl. Instr. and Meth. **A417** (1998) 230.

[34] N. Akopov et al., Nucl. Instr. and Meth. **A479** (2002) 511.

[35] H. Avakian et al., Nucl. Instr. and Meth. **A417** (1998) 69.

[36] P. Liebing, Ph.D. Thesis, (2004) Hamburg University.

[37] C. Shearer, Ph.D. Thesis, (2005) University of Glasgow.

[38] M. Ahmed and T. Gehrmann, Phys. Lett. B **465** (1999) 297

[39] A. Bacchetta and M. Radici, Phys. Rev. D **69**, 074026 (2004)